

## Monte Carlo calculations on $Z_2$ gauge-Higgs theories

Gary A. Jongeward and John D. Stack

*Department of Physics, University of Illinois at Urbana-Champaign, Urbana, Illinois 61801*

C. Jayaprakash

*Baker Laboratory, Cornell University, Ithaca, New York 14853*

(Received 29 February 1980)

Monte Carlo calculations have been carried out on  $Z_2$  lattice gauge theories in  $d = 3$  and  $d = 4$  space-time dimensions. For  $d = 3$ , for the gauge-Higgs system, the results show a phase diagram in which the Higgs and confined regions are smoothly connected. There are lines of phase transitions surrounding the unconfined region; first-order behavior occurs on and near the self-dual line. For  $d = 4$ , for the pure gauge system, we confirm the results of Creutz *et al.*, that the transition between confined and unconfined regions is first order.

### I. INTRODUCTION

In this paper, we report the results of our Monte Carlo calculations on  $Z_2$  lattice gauge theories. The  $Z_2$  gauge theory was first written down long ago by Wegner,<sup>1</sup> as part of a sequence of generalizations of the Ising model. It is currently of interest to particle theorists as a simple gauge theory in which confinement can be studied. When matter fields are present, the  $Z_2$  action can be written

$$S = K \sum_{\underline{x}, \underline{k}, \underline{l}} [1 - U_{kl}(\underline{x})] + h \sum_{\underline{x}, \underline{k}} [1 - \sigma(\underline{x}) U_k(\underline{x}) \sigma(\underline{x} + \underline{k})]. \quad (1)$$

The plaquette variable  $U_{kl}(\underline{x})$  is expressed in terms of the link variable  $U_k(\underline{x})$  by

$$U_{kl}(\underline{x}) = U_k(\underline{x}) U_l(\underline{x} + \underline{k}) U_k(\underline{x} + \underline{k} + \underline{l}) U_l(\underline{x}).$$

Both the link variables  $U_k(\underline{x})$  and the matter variables  $\sigma(\underline{x})$  are restricted to the values  $\pm 1$ . If they were instead allowed to take complex values of the form  $e^{i\theta}$ , the model defined by Eq. (1) would be a lattice version of the Abelian Higgs model.<sup>2</sup> We will keep this resemblance in mind by referring to  $h$  as the Higgs coupling and  $K$  as the gauge coupling. Both are inversely related to the usual field-theory coupling constants. We also refer to the limiting region  $h \rightarrow \infty, K \rightarrow \infty$  as the Higgs region, since for a continuous gauge group this is where the usual Higgs mechanism is operative. The opposite extreme  $h \rightarrow 0, K \rightarrow 0$  will be referred to as the confinement region, since this is where series expansions in  $K$  can be carried out and confinement established.

The model of Eq. (1) is first defined for space-time dimensionality  $d = 2$ . However, by making a Kramers-Wannier duality transformation, this case can be mapped into an Ising model in an external field, a model whose properties have already been fully explored. For  $d = 3$ , the model is self-dual and highly nontrivial.<sup>3</sup> It is related to

previously studied systems only in the limits  $h = 0$  or  $K = \infty$ .

The main focus of our work has been to find the phase diagram of this theory, and to classify the order of the phase transition which occurs along each section of the boundary between phases. Our results for the phase diagram for  $d = 3$  are presented in Sec. III. We find a phase diagram (see Fig. 1) in which the unconfined region is surrounded by lines of phase transitions. These lines are second order until they are quite near each other and the self-dual line, where first-order behavior occurs. First-order behavior continues to occur along the self-dual line for a finite distance, where it terminates, perhaps in a critical point. The Higgs and confinement regions are found to be continuously connected, as required by a theorem proven recently.<sup>4,5</sup> We have also studied the pure gauge system ( $h = 0$ ) for  $d = 4$ . We confirm the strong first-order transition, originally discovered by Creutz *et al.*<sup>6</sup> Our results in both three and four dimensions are in Sec. III. In Sec. II, we give a general overview of the Monte

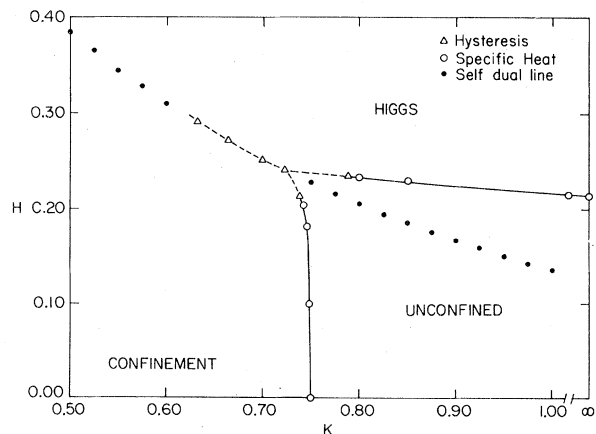


FIG. 1. Phase diagram for the  $d = 3$  gauge-Higgs system ( $GH^3$ ). Dashed lines: first-order transitions. Solid lines: second-order transitions.

Carlo method and how it is used to locate phase transitions, relegating certain mathematical details to the Appendix. Section IV contains concluding remarks.

## II. THE MONTE CARLO METHOD

### A. General description

In the Euclidean formulation, propagators and other quantities of interest in quantum field theory can be obtained by carrying out a calculation in classical equilibrium statistical mechanics. The action of the original field theory becomes the Hamiltonian of the statistical-mechanics system, and after discretizing with a lattice, the Euclidean Feynman path integral becomes the configuration sum which must be evaluated to obtain expected values. Thus for the model defined by Eq. (1) the expected value of a quantity  $O$  is defined by

$$\langle O \rangle = \left[ \sum_{\sigma, \sigma_k} O \exp(-S) \right] / \left[ \sum_{\sigma, \sigma_k} \exp(-S) \right]. \quad (2)$$

At this stage, the number of degrees of freedom in the problem is still infinite. The obvious next step is to approximate the infinite lattice by a finite one.

While possible in principle, direct evaluation of expected values on a finite lattice is impractical, since even for lattices which are only a few sites on a side, the number of configurations needed to evaluate  $\langle O \rangle$  directly is prohibitively large.

The Monte Carlo method replaces direct evaluation by a statistical procedure which can lead to an accurate estimate of  $\langle O \rangle$  for a finite lattice in feasible computing time. The basic physical idea behind the method can be described by first considering a real classical system with a large number of degrees of freedom. Starting from an arbitrary initial state, the system will generally relax into thermal equilibrium. After an initial interval characterized by the relaxation time of the system, a time average of a quantity  $O$  will then be sampling the Boltzmann distribution and as the time increases, the time average of  $O$  will approach the ensemble average of Eq. (2). The important observation of Metropolis and collaborators was that any dynamical scheme can be used, as long as the system is eventually guaranteed to approach equilibrium.<sup>7</sup> The dynamics need not have anything to do with the actual evolution of the system, and in fact for our calculations where the equilibrium situation represents Euclidean quantum field theory, the concept of time evolution has no direct physical meaning. Nevertheless, for computational purposes a fictitious dynamics can be imposed on the system and expected values computed as time averages.

In the Metropolis method, time is a discrete variable, and dynamics is a simple set of rules for changing configurations. For our  $Z_2$  lattice gauge systems, a configuration is a specific assignment of values to the Higgs and link variables associated with each site of the lattice. Referring to the value of  $S$  as the energy, the rule for changing the value of a Higgs or link variable at a given site involves a comparison between the present energy and the new energy gotten by changing the Higgs or link variable being considered. If the new energy  $E'$  is lower than the present energy  $E$ , the change is accepted. On the other hand, if  $E' > E$ , the change is made with probability  $\exp[-(E' - E)]$ . In practice, this is carried out by comparing  $\exp[-(E' - E)]$  to a pseudorandom number  $\xi$ ,  $0 < \xi < 1$ . If  $\exp[-(E' - E)] > \xi$ , the change is made, otherwise not. At this point another site of the lattice is chosen, and the process repeated. In most of our calculations, sites were chosen by cycling through the lattice in a systematic way, although some calculations were also done by randomly choosing the sites. The random choice of sites appeared to have little effect on the final results. A complete cycle through all the Higgs and link variables of the lattice corresponds to what is called in the Monte Carlo literature one Monte Carlo step/spin. We will simply refer to this as one cycle or one step. The calculation of the desired estimate for  $O$  is accomplished by computing the average of  $O$  over the Monte Carlo steps in the calculation. The normalizing integral in the denominator of Eq. (2) is never needed. The number of steps in a given calculation is an important measure of its quality. In principle, it is only the average of  $O$  as the number of steps approaches  $\infty$  which converges to the equilibrium expected value of  $O$ . In practice, an attempt is made to make the number of steps in the calculation significantly exceed the relaxation time or the number required to reach equilibrium for all practical purposes.

Standard proofs are available that a system evolving under Metropolis dynamics eventually reaches the Boltzmann distribution.<sup>8</sup> A heuristic discussion is given in the Appendix. Evidently, the Metropolis scheme is only one of a variety of different possible algorithms, but is one of the most widely used, since it is simple and provides a relatively rapid relaxation to equilibrium. Over the years, an enormous amount of experience has been gained in the use of Monte Carlo methods as applied to Ising and other spin systems of interest to condensed-matter physicists.<sup>9</sup> Of particular interest for our purposes is the fact that Monte Carlo calculations on lattices of moderate size show strong evidence for the phase transitions present in the infinite system.

In a particle-physics context, Wilson first advocated the application of Monte Carlo methods to lattice gauge theories, and is currently carrying out calculations on non-Abelian theories.<sup>10</sup> Subsequently, Creutz *et al.* have carried out and reported on a number of calculations for  $Z_2$  and  $Z_n$  systems,<sup>6</sup> and more recently for non-Abelian theories.<sup>11</sup>

#### B. Monte Carlo and first-order transitions

The hallmarks of a first-order phase transition in a real system are the possibility of phase coexistence, a finite latent heat, and a correlation length which remains finite at the transition. The last property prevents a lattice theory from having a continuum limit at a first-order transition. Closely related to these other characteristics of a first-order transition is the existence of metastable states, analogous to a supercooled gas or a superheated liquid.

In general, the methods used to analyze first-order transitions with Monte Carlo methods are of two types, thermal cycle or hysteresis methods, and quenching. In a thermal cycle, a given coupling is slowly changed, say increased. After a large number of small increments has been carried out, the process is reversed, and the coupling is slowly decreased until the original starting value is reached. If there is a first-order transition between the upper and lower extremes, a plot of a typical energy of the system will show hysteresis in a manner qualitatively similar to the familiar plots of  $B$  vs  $H$  for a magnet. The location of the interval over which hysteresis occurs can be used to estimate the coupling value of the transition, and the discontinuity in energy across the transition similarly gives an estimate of the latent heat. In our  $Z_2$  system, there are two characteristic energy densities: the plaquette energy density  $E_P$ , defined to be the value of  $K[1 - U_{kl}(x)]$ , averaged over all plaquettes of the lattice, and the link energy density  $E_L$ , defined as the value of  $h[1 - \sigma(x)U_r(x)\sigma(x+k)]$ , averaged over all links of the lattice. In Sec. III we give the results of thermal cycles in  $K$  for both  $E_P$  and  $E_L$  at fixed  $h$ . The precise procedure followed is stated there.

The other method commonly used in Monte Carlo studies of first-order transitions is called quenching. Here after allowing the system to reach equilibrium at some initial values of  $K$  and  $h$ , a coupling, e.g.,  $K$ , is suddenly switched to a new value. If the new value lies just beyond a first-order transition, the system will "remember" its starting point, and the energy density will remain at its original value for a large number of Monte Carlo steps before finally relaxing rather quickly to its equilibrium value at the new coupling. Thermal

cycles and quenches are thus different probes for the existence of metastable states. We have found in all our calculations that the two give mutually consistent results. So in the following, we present the information obtained from thermal cycles.

#### C. Monte Carlo and second-order transitions

Second-order, or critical transitions, are characterized by the absence of phase coexistence and metastable states, and have zero latent heat. A thermal cycle should thus show no hysteresis across a critical transition.<sup>12</sup> The correlation length goes to infinity at a critical transition in a real system, which gives rise to diverging fluctuations, and characteristic singular behavior in specific heats, susceptibilities, etc. For a finite lattice, the correlation length cannot exceed the lattice size. This leads to rounding of the singular behavior present for the infinite system. A standard Monte Carlo test for a critical transition is thus to study a specific heat of the system for different lattice sizes. If the infinite system has a critical point with a diverging specific heat, the finite system will have a peaked specific-heat curve which sharpens as lattice size increases. The maximum of the specific heat will approach the critical point of the infinite system as lattice size increases. The theory of how the location of the peak in specific heat scales with lattice size has been worked out in detail by Fisher and collaborators.<sup>13</sup> In Sec. IIIB, we show the results in  $d=3$  of calculations of the link specific heat  $C_L = N_L(\langle E_L^2 \rangle - \langle E_L \rangle^2)$ , where the link energy density is given according to its definition by

$$E_L \equiv \frac{h}{N_L} \sum_{\underline{x}, \underline{k}} [1 - \sigma(\underline{x})U_r(\underline{x})\sigma(\underline{x}+\underline{k})],$$

where  $N_L$  is the number of links of the lattice. To obtain a good value for a specific heat at a given value of couplings usually requires averaging over several thousand Monte Carlo cycles through the lattice. This is due to the large fluctuations characteristic of a critical transition.

Thought of in terms of total energy density, the contrast between first- and second-order transitions is that the first-order case has a discontinuous energy density across the transition, with finite fluctuations on either side, whereas the second-order case has a continuous energy density with large fluctuations which diverge at the critical point for an infinite system. These sharp distinctions are blurred to some extent on a finite lattice, but can be enhanced by increasing lattice size and the statistical quality of the computation.

In Sec. III, we apply the standard methods described above to our  $Z_2$  system for  $d=3$  and  $d=4$ . The first-order transition found for  $d=4$  is more

strongly first order than the first-order region for  $d=3$ . For example, the  $d=4$  system shows unmistakable hysteresis for a  $4^4$  lattice, whereas for the  $d=3$  system, it was necessary to compute on a  $10^3$  lattice to clearly resolve first- and second-order regions.

### III. RESULTS IN THREE AND FOUR DIMENSIONS

In this section we present our results on  $Z_2$  lattice gauge theories, first for the pure gauge system in  $d=4$  dimensions and then for the Higgs-gauge system in  $d=3$  dimensions. Periodic boundary conditions are used in all cases. Our discussion of four dimensions is brief, since this case has already been reported on by Creutz *et al.*<sup>6</sup> Our work provides an independent confirmation of their conclusion that the transition in this case is first order in character and is a good example of a strongly first-order transition. The three-dimensional gauge-Higgs system is more subtle, involving regions of first-order behavior which connect smoothly to second-order regions.

#### A. $d=4$

In four dimensions, the pure gauge theory defined by the action of Eq. (1) with  $h=0$  is self-dual.<sup>3</sup> The coupling  $K^*$  of the dual theory is related to the original coupling  $K$  by  $K^* = -\frac{1}{2} \ln(\tanh K)$ . Assuming a unique phase transition, the coupling at the phase transition must satisfy  $K_c = -\frac{1}{2} \ln(\tanh K_c)$ , which is solved by  $K_c = \frac{1}{2} \sinh^{-1}(1)$ . For  $K < K_c$ , the theory is characterized by electric confinement: The Wilson-loop integral will fall off exponentially in the area of the loop, while for  $K > K_c$ , the loop integral varies with the perimeter of the loop. Since the theory is completely self-dual, the region  $K > K_c$  corresponds to confinement of magnetic charge, and shows an area law for the Wilson loop defined in terms of the dual gauge variables.

In four dimensions, as mentioned above, the transition in the pure gauge theory is first order in character. In Fig. 2, we display a thermal cycle on a  $4^4$  lattice. The procedure was to remain at each value of  $K$  for  $N=40$  complete sweeps through the lattice, then to increase or decrease  $K$  by  $\Delta K$ . The value  $\Delta K = 0.0005$  was used. For the part of the run with  $K$  decreasing, equilibrium was first established at  $K=0.6$ , whereas for  $K$  increasing,  $K=0.3$  was the initial value. The quantity plotted in Fig. 2 is the average plaquette energy density  $\bar{E}_P$  (see Sec. II B for the definition of  $E_P$  and  $E_L$ ), where the bar implies an average over the  $N$  steps at each  $K$ . The quantity  $K[1 - U_{RI}(x)]$  which controls  $\bar{E}_P$  is the analog of the square of field strength  $F_{\mu\nu}$  in the continuum limit of a U(1) theory. For our  $Z_2$  theory this quantity can only take

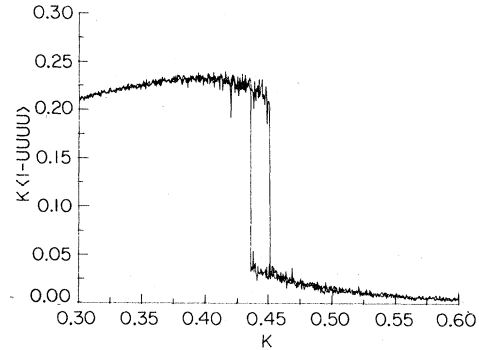


FIG. 2. Thermal cycle in  $K$  of  $\bar{E}_P$  for the  $d=4$  pure gauge system.

two values. Zero field strength corresponds to  $U_{RI}(x) = +1$ , while maximum field strength corresponds to  $U_{RI}(x) = -1$ . For large  $K$ , the state of the system becomes essentially pure gauge with zero field strength on most plaquettes, and  $\bar{E}_P$  is small. This is the unconfined region for electric charge. For the opposite limit of small  $K$  values, there is no strong suppression of plaquettes with nonzero field strength and the energy density  $\bar{E}_P$  is much larger. This is the region of electric confinement. For values of  $K$  away from the phase transition, our Monte Carlo values for  $\bar{E}_P$  agree well with those calculated from series expansions available in the literature.<sup>14</sup>

In Fig. 2, the difference between  $K$  increasing and  $K$  decreasing shows up as clear-cut hysteresis, and provides convincing evidence for a first-order transition. The midpoint of the hysteresis loop is at  $K \cong 0.443$ , which is very close to the value of  $K_c = \frac{1}{2} \sinh^{-1}(1) = 0.441$ , which locates the transition for the bulk system. The curve shown was obtained by cycling through the lattice systematically. We have checked that random cycling has a negligible effect on the results. Quenches from either direction to values of  $K$  just beyond the transition show metastable behavior quite clearly. The metastable behavior is stable against all the perturbations we have tried including random cycles through the lattice and flipping two different links per site.

#### B. $d=3$

We now turn to our results for the  $Z_2$  system with gauge and Higgs variables in  $d=3$ . The basic facts known prior to our work are the following: (1) The model is self-dual<sup>3</sup> with dual couplings  $K^*$ ,  $h^*$  related to original couplings  $K$ ,  $h$  by  $K^* = -\frac{1}{2} \ln[\tanh(h)]$  and  $h^* = -\frac{1}{2} \ln(\tanh K)$ . (2) Known results<sup>15</sup> from the  $d=3$  Ising model imply that there is a critical phase transition on the  $h$  axis at  $h = h_c(K = \infty) = 0.2217$ ; by duality there is

also a critical point on the  $K$  axis at  $K = K_c(h=0) = 0.7613$ . (3) A recently proven rigorous theorem requires that confinement ( $K, h$  small) and Higgs ( $K, h$  large) regions be continuously connected by a region free of phase transitions.<sup>4,5</sup> (4) A theoretical argument given by Wegner<sup>1</sup> suggests that the critical points on the axes are terminating points of critical lines extending into the finite  $h$ - $K$  plane, i.e., that a phase transition second order on the boundary of the phase diagram will remain second order for a finite distance into the interior of the phase diagram.

The presentation of results is organized as follows: We first show the results of thermal cycle or hysteresis runs where  $K$  is either slowly increased or decreased, holding  $h$  at a fixed value. These results serve to map out the region where there is evidence for first-order behavior. Next, we show specific-heat calculations, and compare specific-heat maxima for different lattice sizes to establish regions of second-order behavior. Figure 1 is the simplest phase diagram consistent with our results.

The thermal cycle results presented are for a  $10^3$  lattice, using  $\Delta K = 0.0005$  and  $N = 40$ , just as in the  $d = 4$  case. To conserve computer time, for each value of  $h$ , the region of possible occurrence of a phase transition was located by using larger values of  $\Delta K$  and smaller values of  $N$ , e.g.,  $\Delta K = 0.001$  and  $N = 10$ . The final very slow calculations with  $\Delta K = 0.0005$  and  $N = 40$  were made between a lower value  $K_1(h)$  and an upper value  $K_2(h)$ , with  $K_2(h) - K_1(h) = 0.2$  surrounding this possible phase transition. This value of  $K_2 - K_1$  greatly exceeds the interval in  $K$  over which there is rapid variation of energy density or other significant structure. The quantities plotted are the average plaquette energy density  $\bar{E}_P$  defined in the same way as in  $d = 4$ , and the corresponding average link energy density  $\bar{E}_L$ . The quantity corresponding to  $E_L$  would represent the gauge-invariant photon mass term in the U(1) continuum Higgs model. We have checked that our results for  $\bar{E}_P$  and  $\bar{E}_L$  agree with results from other methods of calculation in the following limits: (1) For large  $K$  ( $K \geq 0.8$ ), and  $h = 0$ ,  $\bar{E}_P$  can be obtained by taking the dual of the high-temperature expansion of the Ising model.<sup>15</sup> In fact, these same values work well at finite  $h$ , showing only mild reduction up to  $h = 0.2$ , which reflects the  $O(h^4)$  nature of the effect of the Higgs coupling in this region.<sup>1</sup> (2) For large  $K$ , ( $K \geq 1.0$ ), the value of  $\bar{E}_L$  is given quantitatively by the Ising-model energy density at coupling  $h$ . This reflects the freezing out of the gauge degrees of freedom for large  $K$ . (3) For small  $K$  and  $h$  ( $K \leq 0.5$ , and  $h \leq 0.3$ ) both  $\bar{E}_P$  and  $\bar{E}_L$  are well represented by high-temperature series available in the liter-

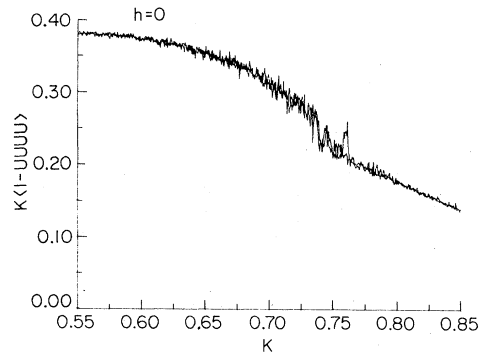


FIG. 3. Thermal cycle in  $K$  at  $h=0$  of  $\bar{E}_P$  for  $\text{GH}^3$ .

ature<sup>14</sup> for  $h=0$ , and extended to finite  $h$  by Jayaprakash.<sup>16</sup> (4) For  $K=0$ ,  $E_L$  is given by  $E_L = 2h/(1+e^{2h})$ .

The most striking feature of the thermal cycles for  $\bar{E}_P$  and  $\bar{E}_L$  shown in Fig. 3–Fig. 10 is the hysteresis which is clearly evident for  $h \geq 0.24$ , and has faded away by  $h \approx 0.30$ . This constitutes strong evidence for first-order behavior in this system. We suspect that the actual onset of first-order behavior occurs at approximately  $h = 0.22$ , but calculations of high quality on a much larger lattice would be required to verify this. For val-

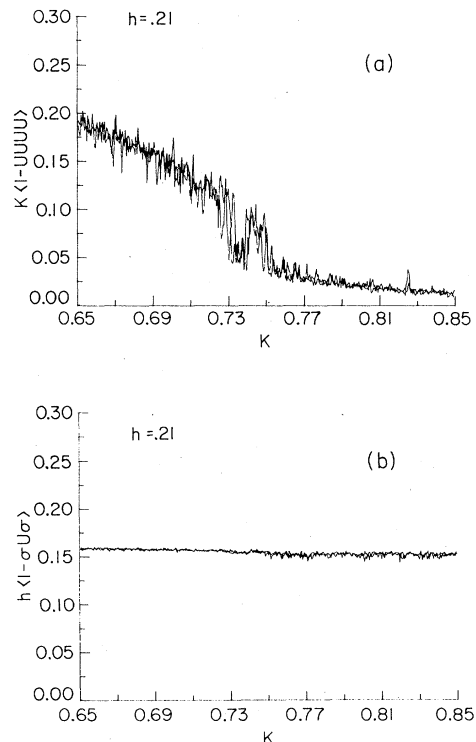


FIG. 4. Thermal cycle in  $K$  at  $h=0.21$  of (a)  $\bar{E}_P$ , (b)  $\bar{E}_L$ , for  $\text{GH}^3$ .

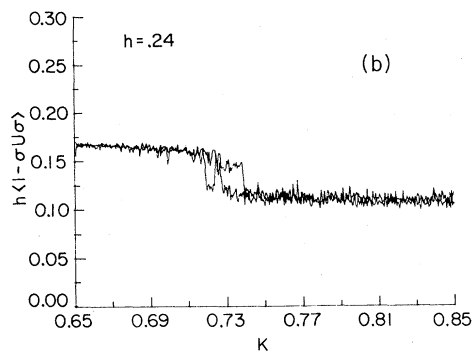
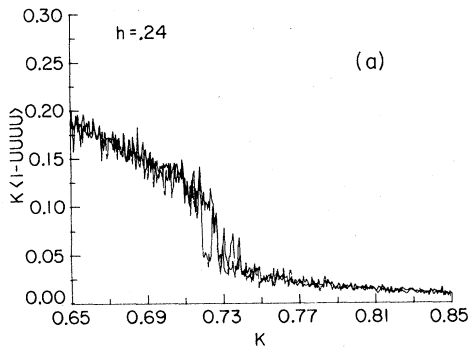


FIG. 5. Thermal cycle in  $K$  at  $h=0.24$  of (a)  $\bar{E}_P$ , (b)  $\bar{E}_L$ , for  $\text{GH}^3$ .

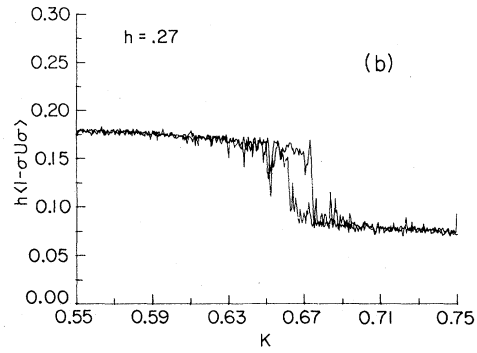
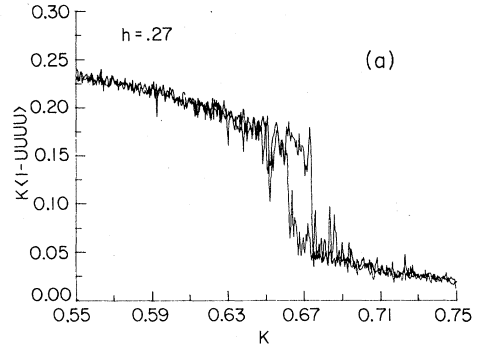


FIG. 7. Thermal cycle in  $K$  at  $h=0.27$  of (a)  $\bar{E}_P$ , (b)  $\bar{E}_L$ , for  $\text{GH}^3$ .

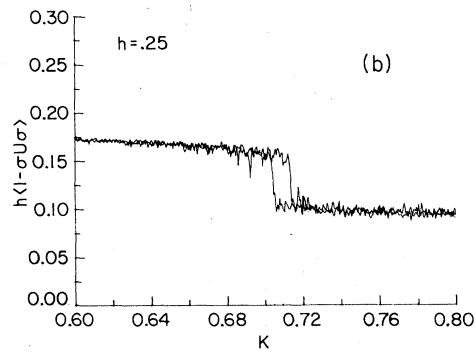
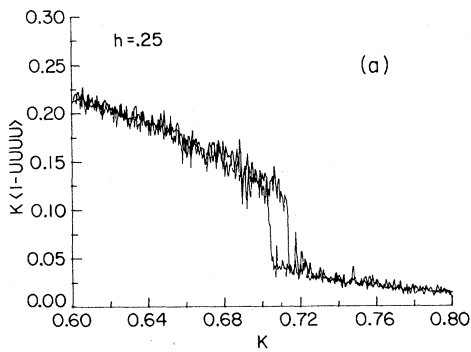


FIG. 6. Thermal cycle in  $K$  at  $h=0.25$  of (a)  $\bar{E}_P$ , (b)  $\bar{E}_L$ , for  $\text{GH}^3$ .

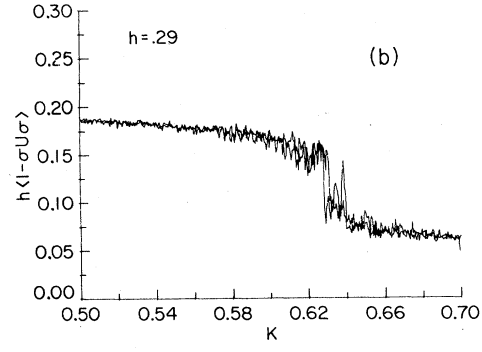
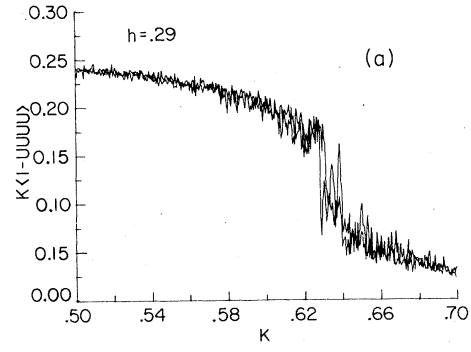


FIG. 8. Thermal cycle in  $K$  at  $h=0.29$  of (a)  $\bar{E}_P$ , (b)  $\bar{E}_L$ , for  $\text{GH}^3$ .

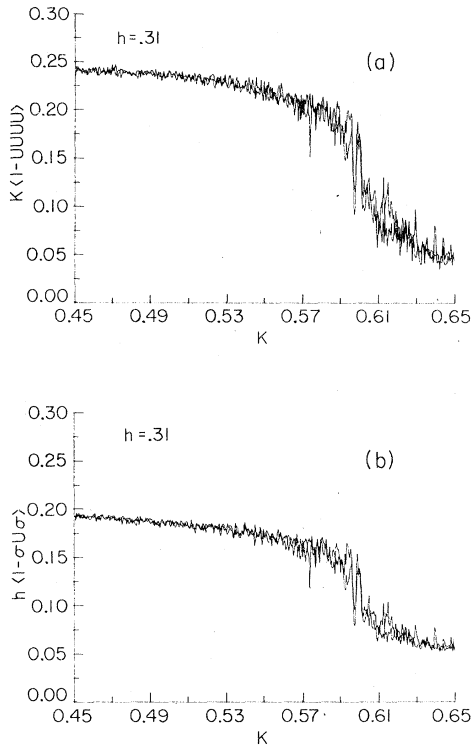


FIG. 9. Thermal cycle in  $K$  at  $h=0.31$  of (a)  $\bar{E}_P$ , (b)  $\bar{E}_L$ , for  $\text{GH}^3$ .

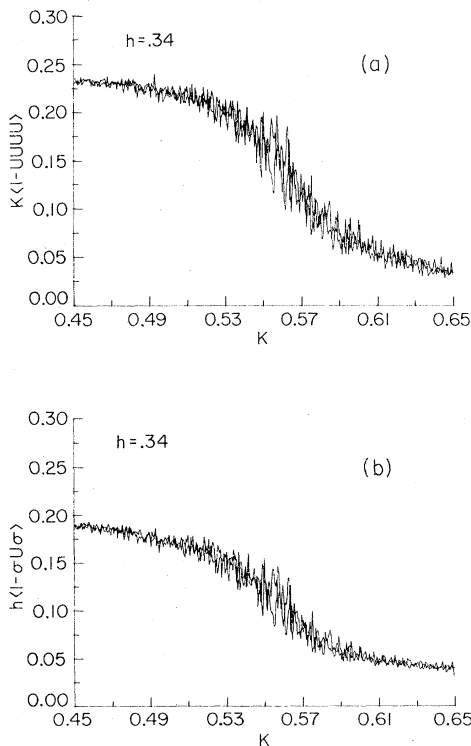


FIG. 10. Thermal cycle in  $K$  at  $h=0.34$  of (a)  $\bar{E}_P$ , (b)  $\bar{E}_L$ , for  $\text{GH}^3$ .

ues of  $h$  greater than 0.30, there is no sign of any further first-order behavior, although there are large fluctuations in both  $E_P$  and  $E_L$  in the region connecting low and high  $K$  values. We have made several sweeps at much larger values of  $h$  and found no significant structure of any kind. In our calculations, the Higgs and confinement regions are truly connected.

To study the possibility of second-order or critical phase transitions, we have compared the maxima in specific heat curves for  $d=3$  cubic lattices with 6, 8, and 10 sites on a side. While our thermal cycle calculations were done in the "gauge" mode, moving the value of  $K$  at fixed  $h$ , the specific-heat calculations were done in the "Higgs" mode, moving the value of  $h$  at fixed  $K$ . While by duality the two are ultimately equivalent, there is a computational advantage to calculating in the Higgs mode. The reason can be seen as follows: The critical transition on the  $K$  axis occurs at  $K=0.7613$ . The line of critical transitions which extends to  $h>0$  from the critical point on the  $K$  axis lies in the interval  $0.7 \leq K \leq 0.76$  for  $0 \leq h \leq 0.2$ . The dual of this region corresponds to  $0.252 \geq h \geq 0.222$  and  $\infty \geq K \geq 0.811$ . For these large values of  $K$ , the plaquettes are not strongly fluctuating and the system is dominated by the link behavior. We have found that in this dual region, the Monte Carlo procedure produces good values for the total link energy and its fluctuations in less computing time than it does for the total plaquette energy density and its fluctuations in the original region. This is not surprising, since although it produces self-dual values, the Metropolis algorithm is not itself a self-dual procedure.

In Figs. 11 and 12, we show the behavior of the link specific heat  $C_L$  defined in Sec. IIC for different size lattices. The values shown are the averages of two runs, both consisting of 8000 complete steps through the lattice at value of  $h$ . To ensure equilibrium, an initial set of 8000 steps was eliminated. The  $K = \infty$  curves are of course just the  $d=3$  Ising model and our values agree well with those of Landau.<sup>17</sup> The curves for  $K=0.85$  are qualitatively similar. Both cases show the typical sharpening of the peak expected for a critical transition as the lattice size increases. We have checked that our results are consistent with finite-scaling analysis, but without results from one very large lattice, e.g.,  $25^3$ , we cannot give more than rough estimates for critical exponents.

In Fig. 1, we give the simplest phase diagram consistent with our results. We have used the centers of the hysteresis curves to locate the first-order transitions, and used the maximum in specific heat for the  $10^3$  lattice to locate second-order transitions. These latter values of course differ

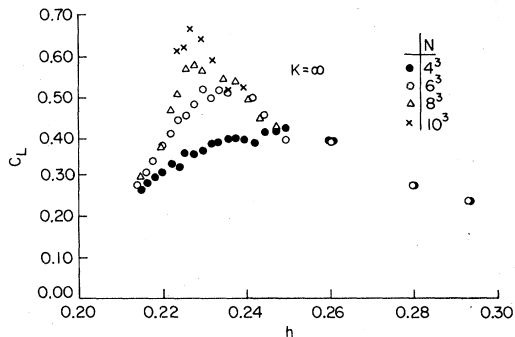


FIG. 11. Specific heat  $C_L$  vs  $h$  for  $K=\infty$  on  $6^3$ ,  $8^3$ , and  $10^3$  lattices.

from the true values expected for a bulk system by finite-size effects. For example, the Ising transition which should be at  $h=0.2217$  ( $K=\infty$ ) is instead at  $h=0.2275$  from the  $10^3$  specific-heat maximum. The curves between the points located by the specific heat maxima of Figs. 11 and 12 are supported by less extensive specific-heat calculations. For the first-order transitions, the centers of the hysteresis loops for  $h \geq 0.24$  fall very close to or on the self-dual line  $h = -\frac{1}{2} \ln(\tanh K)$ . Finite-size effects are less crucial for first-order transitions, so these values are more likely to apply to the bulk system.

We are confident of the following main features of the phase diagram of Fig. 1: (1) Both first- and second-order behaviors are present in this system. (2) Higgs and confinement regions are smoothly connected. (3) The unconfined region is completely separated from the rest of the diagram by lines of phase transitions. A detailed question which deserves further study is the precise nature of the switchover from critical to first-order behavior which occurs near the self-dual line. It is not ruled out, for example, that the critical lines which come off the  $h$  and  $K$  axes remain critical all the way to the self-dual line. The question of whether the first-order behavior on the self-dual

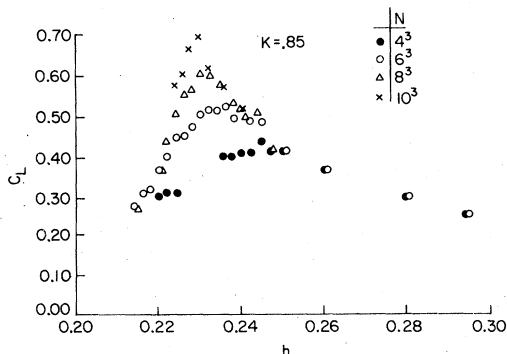


FIG. 12. Specific heat  $C_L$  vs  $h$  for  $K=0.85$  on  $6^3$ ,  $8^3$ , and  $10^3$  lattices.

line terminates in a critical point at  $h \sim 0.3$ ,  $K \sim 0.62$  also deserves further study.

#### IV. CONCLUSIONS

We have found Monte Carlo calculations to be a versatile and useful method for locating and classifying phase transitions. Although by itself the  $Z_2$  system we studied is too simple to be a realistic model in particle physics, it has been suggested by 't Hooft<sup>18</sup> that the  $Z_2$  theory is relevant to the analysis of  $SU(2)$  lattice gauge theories, since  $Z_2$  is the center of the group  $SU(2)$ .

Our results in  $d=3$  dimensions for the  $Z_2$  gauge-Higgs system show a phase diagram with surprisingly rich structure. Although expected whenever Higgs and gauge variables transform in the same way,<sup>4</sup> it is nonetheless striking to see a concrete example where Higgs and confinement regions are continuously connected. It is also noteworthy that the theoretical argument of Wegner<sup>1</sup> is valid in this model over a wide range. The Higgs coupling  $h$  not only fails to destroy the transition separating confined and unconfined regions for infinitesimal  $h$ , but in fact the transition survives with little change in its character up to  $h \sim 0.22$ . Finally, the fact that there is first-order behavior in this system was at least to us, unexpected. It would clearly be of interest to gain insight into the mechanisms which cause a critical transition to continuously "harden" and finally become first order.

#### ACKNOWLEDGMENTS

The work of G. Jongeward and J. Stack was supported in part by the National Science Foundation under Grant No. NSF PHY 79-00272. The work of C. Jayaprakash was also supported in part by the National Science Foundation. We would also like to thank the University of Illinois Research Board for a grant of computing time.

#### APPENDIX

Starting from an initial configuration  $x_0$ , we sequentially apply the Metropolis algorithm to generate new configurations  $x_1, \dots, x_N$ . Let  $P_N(x)$  be the probability that  $x_N = x$  after  $N$  steps in the sequence, where  $x$  is an arbitrary configuration. What we want to make plausible is that as  $N \rightarrow \infty$ ,  $P_N(x) \rightarrow ce^{-E(x)}$ , where  $c$  is a normalizing constant.

The probability after  $N+1$  steps is related to  $P_N(x)$  by



$$\begin{aligned}
P_{N+1}(x) &= \sum_{x'} W(x' \rightarrow x) P_N(x') + \left(1 - \sum_{x'} W(x \rightarrow x')\right) P_N(x) \\
&= P_N(x) + \sum_{x'} [P_N(x') W(x' \rightarrow x) - P_N(x) W(x \rightarrow x')] ,
\end{aligned} \tag{A1}$$

where  $W(x \rightarrow x')$  is the probability for the transition  $x \rightarrow x'$ .

From Eq. (A1), it is clear that  $P_N(x)$  satisfying

$$P_N^{\text{eq}}(x) W(x \rightarrow x') = P_N^{\text{eq}}(x') W(x' \rightarrow x) \tag{A2}$$

will be a stationary probability distribution satisfying  $P_{N+1}(x) = P_N(x)$ .

The distribution  $P^{\text{eq}}(x)$  is also stable in that if

$$\frac{P_N(x_a)}{P_N(x_b)} > \frac{W(x_b \rightarrow x_a)}{W(x_a \rightarrow x_b)},$$

then after an iteration of the Metropolis algorithm  $P_{N+1}(x_a) < P_N(x_a)$  and  $P_{N+1}(x_b) > P_N(x_b)$ .

This means that each successive iteration brings  $P_N(x)$  closer to satisfying Eq. (A2), and therefore  $P_N$  asymptotically will approach  $P^{\text{eq}}(x)$ .

At the  $N$ th step in the Metropolis method, one considers the possibility of transitions between the present state  $x$  and a fixed state  $x'$ . The transition occurs with probability  $W(x \rightarrow x')$  defined by

$$W(x \rightarrow x') = \begin{cases} 1, & E(x) > E(x') \\ e^{-[E(x') - E(x)]}, & E(x) < E(x') \end{cases}$$

and thus from Eq. (A2)  $P^{\text{eq}}(x) = ce^{-E(x)}$ . Q.E.D.

<sup>1</sup>F. Wegner, *J. Math. Phys.* **12**, 2259 (1971).

<sup>2</sup>P. W. Higgs, *Phys. Rev.* **145**, 1156 (1966). The lattice version is discussed for example in Ref. 4.

<sup>3</sup>R. Balian, J. M. Drouffe, and C. Itzykson, *Phys. Rev. D* **11**, 2098 (1975). A very readable older reference on duality is G. H. Wannier, *Rev. Mod. Phys.* **17**, 50 (1945).

<sup>4</sup>E. Fradkin and S. Shenker, *Phys. Rev. D* **19**, 3682 (1979).

<sup>5</sup>R. Marra and S. Miracle-Sole, *Commun. Math. Phys.* **67**, 233 (1979).

<sup>6</sup>M. Creutz, L. Jacobs, and C. Rebbi, *Phys. Rev. Lett.* **42**, 1390 (1979), and *Phys. Rev. D* **20**, 1915 (1979); see also M. Creutz, *ibid.* **21**, 1006 (1980).

<sup>7</sup>N. Metropolis, A. W. Rosenbluth, M. N. Rosenbluth, A. H. Teller, and E. Teller, *J. Chem. Phys.* **21**, 1087 (1953).

<sup>8</sup>See, e.g., *Monte Carlo Methods*, edited by J. M. Hammersley and D. C. Handscomb (Methuen, London, 1964).

<sup>9</sup>For a review, see K. Binder, in *Phase Transitions and Critical Phenomena*, edited by C. Domb and M. S.

Green (Academic, New York, 1976), Vol. 5B.

<sup>10</sup>K. Wilson, in *Current Trends in the Theory of Fields*, AIP Conference Proceedings No. 48, Particles and Fields Subseries No. 15 (AIP, New York, 1978), and Cornell Report No. CLNS/80/442, 1980 (unpublished).

<sup>11</sup>M. Creutz, *Phys. Rev. D* **21**, 2308 (1980).

<sup>12</sup>In practice, this is complicated by the phenomenon of critical slowing down, discussed for example by P. C. Hohenberg and B. I. Halperin, *Rev. Mod. Phys.* **49**, 481 (1977).

<sup>13</sup>M. E. Fisher, in *Proceedings of the International Summer School "Enrico Fermi," Course LI* (Academic, New York, 1971); see also M. E. Fisher and M. N. Barber, *Phys. Rev. Lett.* **28**, 1516 (1972).

<sup>14</sup>R. Balian, J. M. Drouffe, and C. Itzykson, *Phys. Rev. D* **11**, 2104 (1975).

<sup>15</sup>M. Fisher and D. S. Gaunt, *Phys. Rev.* **133**, A225 (1964).

<sup>16</sup>C. Jayaprakash (unpublished).

<sup>17</sup>D. P. Landau, *Phys. Rev. B* **14**, 255 (1976).

<sup>18</sup>G. 't Hooft, *Nucl. Phys.* **B138**, 1 (1978).